STATIC AEROELASTIC EFFECTS ON THE AERODYNAMICS OF THE SAAB 37 VIGGEN AIRCRAFT, A COMPARISON BETWEEN CALCULATIONS, WINDTUNNEL TESTS AND FLIGHT TESTS

J. Kloos* and L. Elmeland**
Aerospace Division, SAAB-SCANIA AB
Linköping, Sweden

Abstract

The methods for calculating static aeroelastic effects on the aerodynamics of the canard configuration of the Viggen are presented. They consist of a vortex lattice method for subsonic speeds and a panel method for supersonic speeds. A simple method to account for the effects of mass loading on the aerodynamics of an elastic aircraft is also presented.

Windtunnel tests were used as a check on the calculation methods and for interpolation through the transonic speed range, where calculations cannot be made. The comparison between calculation and windtunnel results is shown.

Finally, flight test results are presented and compared with the results of calculations and windtunnel tests.

Introduction

The requirements for the Saab 37 Viggen aircraft called for one basic configuration, to be developed into attack, reconnaissance, fighter and trainer versions, comprising an unusually wide range of operating conditions, including STOL-characteristics.

To fulfil these requirements the short-coupled canard configuration was chosen, consisting of two thin delta-shaped wings, Figure 1. In such a configuration, aeroelastic effects on the aerodynamic characteristics have to be expected at the high dynamic pressures for which the aircraft has to be designed. Early in the design stage it became moreover clear that not only must aeroelastic effects be taken into account but stiffness requirements had to be quantified to ensure satisfactory flying qualities at high dynamic pressures.

Early in the design work, time is precious and data have limited accuracy, so fairly simple computation methods were put to use to determine the aeroelastic effects on the aerodynamics of the aircraft. Except for minor modifications, mainly consisting of an increase of the number of panels used, especially on the canard, these methods were used throughout the design work and proved, when used as described in this paper, to predict the aeroelastic effects with a fully adequate accuracy, even when compared with flight rest results.

FIGURE 1. SAAB 37 VIGGEN

Calculations

The aeroelastic effects have been calculated with the aid of the influence coefficient method. The airplane is devided into small panels and linearized theory is used to give the coupling between panel airload and the panel angle of attack

$$\{\ell\} = q\,[A]\,\{\alpha\} \qquad (1)$$

where $[A]$ is the aerodynamic influence coefficient matrix.

The airloads cause a structural deformation of the wing, changing the angle of attack

$$\{\Delta\alpha\} = [D]\,\{\ell\} \qquad (2)$$

where $[D]$ is the deformation matrix.

The angle of attack of the panel is composed of two parts: $\{\alpha_o\}$ initial (rigid) value of the wing and $\{\Delta\alpha\}$ due to the aeroelastic deformation

$$\{\alpha\} = \{\alpha_o\} + \{\Delta\alpha\} \qquad (3)$$

* Chief Aerodynamicist
** Supervisor Aerodynamics

From these three equations the angle of attack of the panels in the deformed elastic wing can be obtained

$$\{\alpha\} = \left[[1] - q\,[A][D]\right]^{-1} \cdot \{\alpha_o\} \qquad (4$$

and consequently the loading by combining (1) and (4).

The aerodynamic matrix [A] is for subsonic speed based on the vortex lattice method, ref 1. The panel load is simulated by a swept bound horseshoe vortex placed along the local quarter chord of the panel. The flow tangency requirement is fulfilled at control points positioned at 75% mid chord of each panel, see Figure 2. These positions are chosen because they are correct for a straight two-dimensional airfoil and give good agreement with other theories for simple configurations. For the deformation matrix [D], point loads are placed at 25% panel mid chord and the deflections are given at the control points.

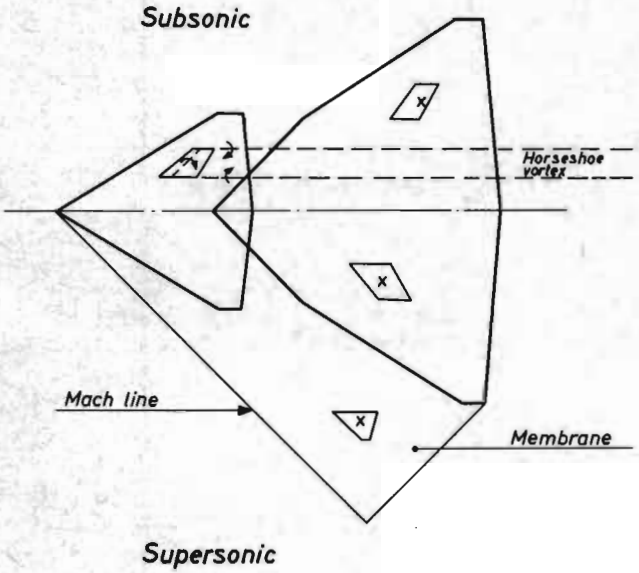

FIG. 2 PANELLING PRINCIPLES

For the supersonic case a method developed by Woodward is used. Each panel is represented by a constant strength source distribution. Building the model starts by producing a configuration with supersonic or sonic edges limited by Mach lines through the extremitics of the wings, see Figure 2. Panels are then placed on the wings and also on a membrane outside the wings inside the limiting edges. These latter panels are eliminated by the condition that their loads are zero. The control points are placed at the panel c.g.'s.

The effect of panel thickness is omitted. This is done as within linearized theory the load consists of two independent parts: load due to angle of attack and load due to thickness. For the calculation of the aerodynamic derivatives, which is our object here, only angle of attack loads and their variation with q and M are needed.

Different calculation models have been used for different purposes as it in this way is possible to greatly reduce the number of panels and consequently computer time. The models give a very simplified picture of the airplane configuration. In the calculation of the pitch derivatives the body has been neglected and the canard and wing extended to the center line, see Figure 3. This is justified by two reasons: the body of this airplane can be considered to be rigid and the loading on the wings is affected only at the inner parts where the deformation is small. The schematisation will of course affect some of the derivatives and its consequences must be kept in mind when applying the results. For instance, $C_{m\alpha}$ and center of pressure are affected but not $C_{L\alpha}$. The calculated c.p. movement and $C_{L\alpha}$ change due to aeroelasticity combined with the rigid-wind tunnel measured-values of c.p. and $C_{L\alpha}$ will then give the wanted aeroelastic coefficients. Another example of simplifications used is given in Figure 4. The body is here represented by a tube. This model has among other things been used for calculation of side force due to aileron deflection.

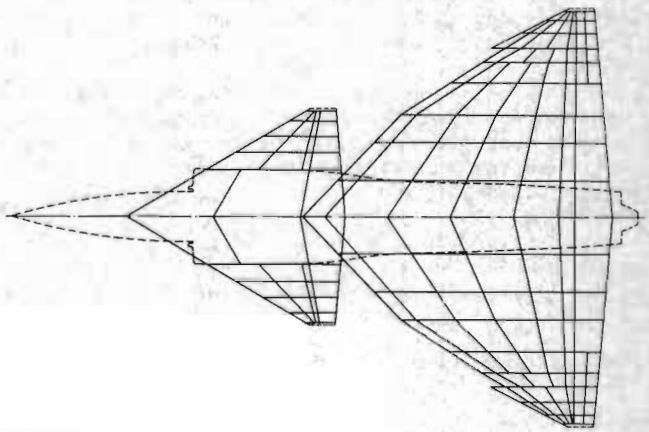

FIGURE 3. CALCULATION MODEL FOR PITCH DERIVATIVES SUBSONIC SPEEDS

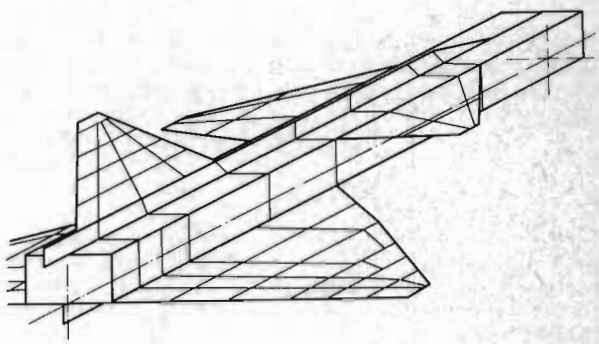

FIGURE 4. CALCULATION MODEL FOR DERIVATIVES INVOLVING COUPLING BETWEEN PITCH AND YAW, SUBSONIC SPEEDS

The panel distribution used is not quite satisfactory from the aerodynamic point of view as the panel size ought to vary in a continuous manner. The distribution was chosen because the structural elastic matrix was originally available only at a limited number of points. The effect of the panel distribution and the number of panels have of course been investigated for different angle of attack distributions but only small and acceptable effects have been found.

The load and control points for which the deformation matrix [D] is needed, do, for several reasons, not always coincide with the points where these quantities are needed. The load and control points are different for the subsonic and supersonic computation, and they are not always suitably located with regard to the structural computation model or suitable for loading or measuring in tests, the latter being especially valid for the elastic windtunnel models.

Therefore the matrices that are needed are computed from available material, computation- or test results, by approximating deformations by spline surface fitting, combining load cases linearly and using Maxwell's reciprocity theorem. In this process the linear deformations are used. The angular deformations that are sought are obtained by differentiating at the end of the process. To obtain angular deformations of adequate accuracy careful measurements and a very strict treatment of the material is necessary.

The most efficient way of organising the aerodynamic data for the elastic aircraft for further use in computing programs proved to be to compile the data for the rigid aircraft as is usually done with aerodynamic data, e.g. $C_N=f(\alpha,\delta_e)$, $C_m=f(\alpha,\delta_e)$, $C_n=f(\beta,\delta_r)$ etc, for different Mach numbers (including an adequate number of cross plots), and then to treat the effect of elasticity separately by introducing an elastic "effectiveness"

η, defined as

$$\eta_{C_{N_\alpha}} = \frac{C_{N_\alpha \text{ elastic}}}{C_{N_\alpha \text{ rigid}}} \quad , \quad \eta_{C_{N\delta_e}} = \frac{C_{N\delta_e \text{ elastic}}}{C_{N\delta_e \text{ rigid}}} \quad \text{etc,}$$

where both the elastic and the rigid derivatives are computed values. Each η is then a function of Mach number M and dynamic pressure q only. This enables an efficient determination of aerodynamic properties of the elastic aircraft for any flight condition. An example of an η-plot is given in Figure 5.

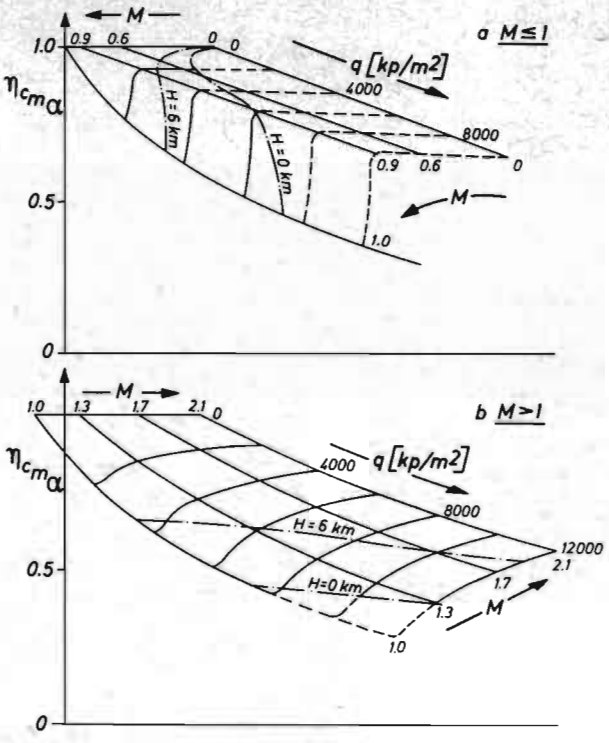

FIG. 5 TYPICAL η-PLOT

Mass loads

When using the aerodynamic data in the way described above, correcting every single coefficient or derivative for elasticity and then using the data in rigid aircraft equations the deformation due to the mass loads has to be taken into account separately.

Load factors and angular accelerations cause deformations of the aircraft structure and consequently add air loads. New derivatives have to be added and how this can be done without introducing new terms into the equations will be shown here with the pitching moment equation as an example.

$$I_y \cdot \dot{q} = \tfrac{1}{2}\rho V^2 S\, c\, (C_{m_o} + C_{m_\alpha}\alpha + C_{m_{\delta_e}}\cdot\delta_e + C_{m_q}\cdot\frac{qc}{2V} + C_{m_{\dot\alpha}}\frac{\dot\alpha c}{2V} + \frac{\partial C_m}{\partial n_z}\cdot n_z + \frac{\partial C_m}{\partial \dot q}\cdot\dot q) \qquad (5)$$

Introducing

$$n_z = 1 + \frac{V}{g}\dot\gamma = 1 + \frac{V}{g}(\dot\theta - \dot\alpha) = 1 + \frac{1}{g}(q - \dot\alpha) \qquad (6)$$

and

$$i_y = \frac{8 I_y}{\rho S c^3} \qquad (7)$$

and regrouping the terms one obtains:

$$\frac{\dot q c^2}{4V^2}\left(i_y - \frac{\partial C_m}{\partial \dot q}\frac{4V^2}{c^2}\right) = C_{m_o} + C_{m_\alpha}\alpha + C_{m_{\delta_e}}\cdot\delta_e + \frac{qc}{2V}\left(C_{m_q} + \frac{\partial C_m}{\partial n_z}\cdot\frac{2V^2}{cg}\right) + \frac{\dot\alpha c}{2V}\left(C_{m_{\dot\alpha}} - \frac{\partial C_m}{\partial n_z}\frac{2V^2}{cg}\right) + \frac{\partial C_m}{\partial n_z} \qquad (8)$$

Naming $C_{m_{\dot q}} = \dfrac{\partial C_m}{\partial\left(\frac{\dot q c^2}{4V^2}\right)}$ and $C_{m_{n_z}} = \dfrac{\partial C_m}{\partial\left(\frac{n_z g c}{2V^2}\right)}$ and

deleting the single $\dfrac{\partial C_m}{\partial n_z}$ term, which is neglectable for the Saab 37, the pitching moment

equation becomes:

$$\frac{\dot{q}c^2}{4V^2}(i_y - C_{m_{\dot{q}}}) =$$

$$C_{m_o}+C_{m_\alpha}\alpha+C_{m\delta_e}\cdot\delta_e+\frac{qc}{2V}(C_{m_q}+C_{mn_z})+\frac{\dot{\alpha}c}{2V}(C_{m_{\dot{\alpha}}}-C_{mn_z}) \quad (9)$$

Treating the normal load equation in the same manner, neglecting $C_{N_{\dot{q}}}$ which is very small, corrected values are obtained for $C_{N_{\dot{\alpha}}}$, C_{N_q}, $C_{m_{\dot{\alpha}}}$, C_{m_q} and i_y which, if they are used in the equations instead of the original values, take the influence of the mass loads on the deformation of the elastic aircraft into account. The corrections are shown in Figure 6 together with numerical values for the Saab 37 at M=.8, sea level. (The values of $C_{N_{\dot{\alpha}}}$ etc are already corrected for elasticity effects i.e. multiplied by their respective η-values). As can be seen the corrections are appreciable in size, but as $C_{m_{\dot{\alpha}}} + C_{m_q}$ is unaffected, damping is affected much less than would be expected at first glance.

Correction for mass loads	Numerical values for Saab 37 at M=.8, sea level
$(C_{N_{\dot{\alpha}}})_{corr} = C_{N_{\dot{\alpha}}} - C_{Nn_z}$	-2.7 = 1.4 - 4.1
$(C_{N_q})_{corr} = C_{N_q} + C_{Nn_z}$	7.3 = 3.2 + 4.1
$(C_{m_{\dot{\alpha}}})_{corr} = C_{m_{\dot{\alpha}}} - C_{mn_z}$	.8 = -.5 + 1.3
$(C_{m_q})_{corr} = C_{m_q} + C_{mn_z}$	-2.7 = -1.4 - 1.3
$(i_y)_{corr} = i_y - C_{m_{\dot{q}}}$	39.9 = 41.6 - 1.7

FIGURE 6. CORRECTIONS FOR MASS LOADS

The typical order of magnitude of the effect of the mass loads on the Saab 37 characteristics at sea level is:

5 - 10% increase of elevator angle per g

10- 15% increase in natural frequency in pitch

0 - 10% decrease in pitch damping

Thus, although the influence of the mass loads is by no means overwhelming, the effect cannot be neglected when comparing computed flight characteristics with flight test results.

Windtunnel tests

An aircraft of the A/C 37 category will experience its largest aeroelastic effects at zero altitude somewhere in the speed region between M=1 and top speed. Here in the transonic region the linear theory is unreliable and the interpolation between subsonically and supersonically calculated results is difficult and must be guided by experiments.

Windtunnel tests have therefore been used as an aid, and this was done in two different ways. Firstly, the results of pressure measurements were used for an empirical correction of the linear theory and secondly, tests on elastic models were performed.

The investigation of the effect of an empirical correction of the linear theory around the transonic speed range has been reported in ref 2.

According to linear theory the panel loads are

$$\{\ell\} = q\,[A]\,\{\alpha\} \quad (1)$$

From windtunnel tests, load distributions are available for two cases that can be used for empirical correction of the [A] matrix, namely loads due to aircraft angle of attack and due to elevon angle. Two coefficients, k and c, are introduced into the matrix:

$$\begin{Bmatrix}\ell_1\\ \ell_2\\ \cdot\\ \cdot\\ \cdot\\ \ell_p\\ \ell_{p+1}\\ \cdot\\ \cdot\\ \ell_n\end{Bmatrix} = q\begin{bmatrix} k_1a_{11}\cdots k_1a_{1p}, c_1a_{1p+1}\cdots c_1a_{1n}\\ k_2a_{21}\cdots k_2a_{2p}, c_2a_{2p+1}\cdots c_2a_{2n}\\ \\ \\ \\ \\ k_na_{n1}\cdots k_na_{np}, c_na_{np+1}\cdots c_na_{nn}\end{bmatrix}\begin{Bmatrix}\alpha_1\\ \alpha_2\\ \\ \\ \alpha_p\\ \alpha_{p+1}\\ \\ \\ \alpha_n\end{Bmatrix} \quad (10)$$

wing panels | elevon panels

The k-values apply to the angle of attack case, chosen with $\delta_e = -\alpha$ so that $\alpha_{p+1} \ldots \alpha_n = 0$, the c-values apply to the elevon angle case.

If linear theory were correct, all the k:s and c:s would be ones. That this is not the case is shown in Figure 7, which shows the k-values for M=0.9. Some values are close to one but some deviate considerably.

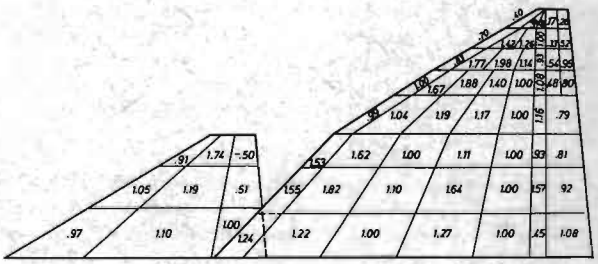

FIG. 7 EMPIRICAL WING INFLUENCE FACTOR k FOR THE ANGLE OF ATTACK CASE AT M=0.9

The aeroelastic effects are recalculated with the corrected matrices. A result is shown in Figure 8. The effect of the correction is not significant in this nor in other cases, an unexpected outcome in view of the k- and c-values. As a consequence, the uncorrected [A] matrices have been used throughout for the aeroelastic calculations.

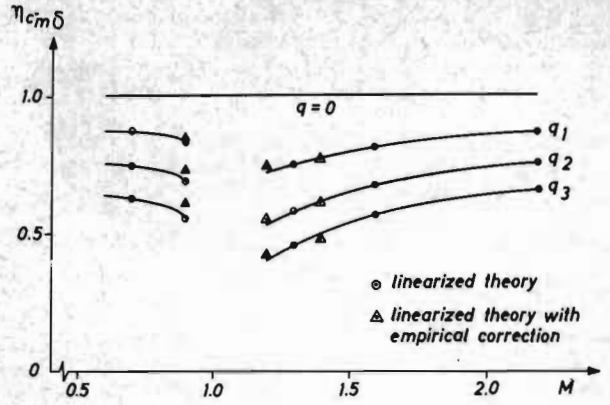

FIGURE 8. INFLUENCE OF EMPIRICAL CORRECTION ON THE COMPUTED AEROELASTIC EFFECTS ON ELEVON EFFECTIVENESS

The windtunnel tests with elastic models were performed with the dual purpose of checking the computation of the η-values and of aiding the interpolation through the transonic speed range.

Three elastic windtunnel models were manufactured. For the first model, scale 1:50, wing, canard and fin were manufactured by milling an approximation of the structure with mainly plane contours. The right aerodynamic contour was obtained by filling with silicone rubber. On the second and third models, 1:50 and 1:30, a better aerodynamic contour was obtained by manufacturing each surface in two halves that were milled to the right outside contour. These halves were also milled from the inside, leaving spars and ribs, Figure 9. By using magnesium, usable dimensions were obtained with a minimum skin thickness of .11 mm. After filling with foamed plastic, the halves were bonded together. Elevons and rudder were made by plating ABS-plastic with copper and nickel.

The models were designed as an approximation of the actual structure with scaled skin thickness and with spars and ribs representing the bending stiffness of the actual spars and ribs, often simplified by lumping a few of them together. In Figure 10 deformations of the main wing structure at three spanwise stations under load are compared with windtunnel model deflection under the same loading.

A check on the η-computations was obtained by measuring the stiffness of the model and computing the η-values for the model as well as measuring them in the windtunnel.

The result of the computations was generally in good agreement with windtunnel test results, an example being shown in Figure 11. The stiffnesses of the left and right model wings were slightly different, so computations were done with both matrices.

Also when non-linearities are involved, the use of η-values for correction for airframe elasticity effects works properly. The aerodynamic data are corrected by using the η-values in the following way:

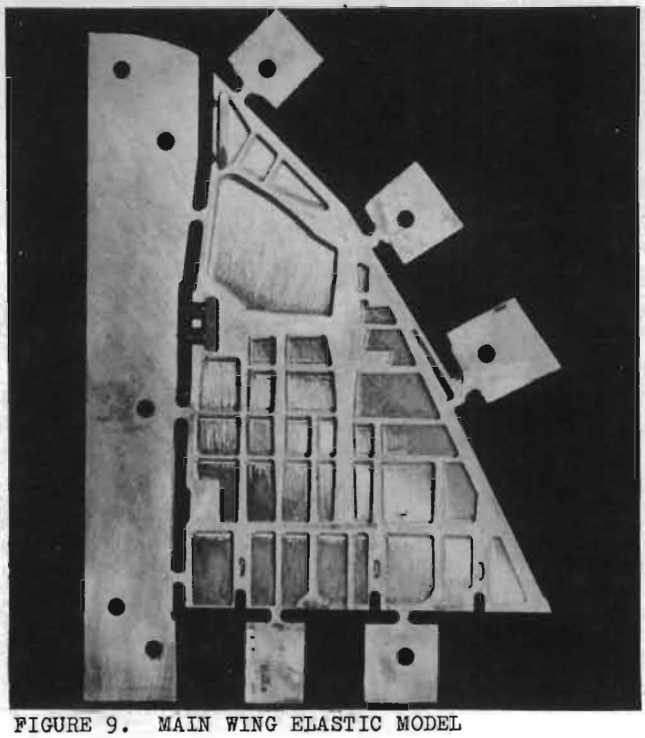

FIGURE 9. MAIN WING ELASTIC MODEL

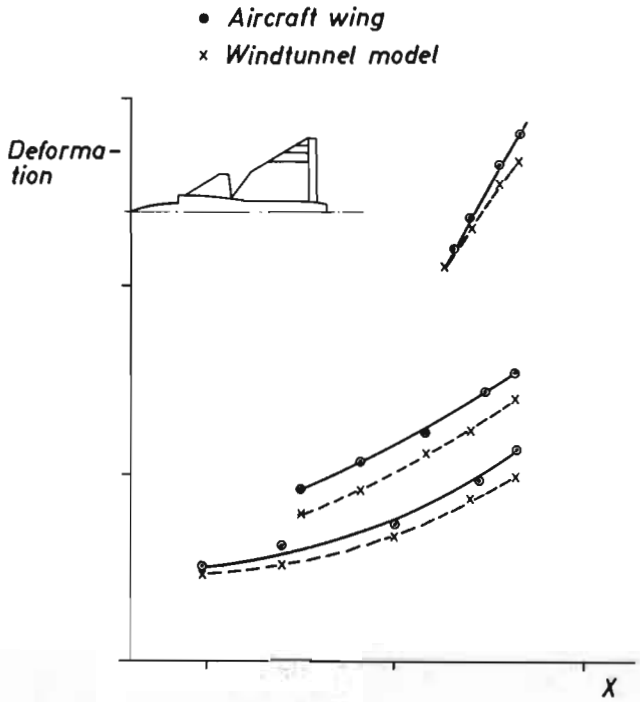

FIG. 10 COMPARISON OF DEFORMATIONS OF AIRCRAFT WING AND WINDTUNNEL MODEL

$$\left\{c_m\ (\alpha_1,\delta_{e1})\right\}_{el} = \left\{c_m\ (0,0)\right\}_r + \left\{\Delta c_m\ (0,0)\right\}_{el} + \eta c_{m_\alpha}\left[\left\{c_m\ (\alpha_1,0)\right\}_r - \left\{c_m\ (0,0)\right\}_r\right] + \eta c_{m_{\delta e}}\left[\left\{c_m\ (\alpha_1,\delta_{e1})\right\}_r - \left\{c_m\ (\alpha_1,0)\right\}_r\right] \quad (11)$$

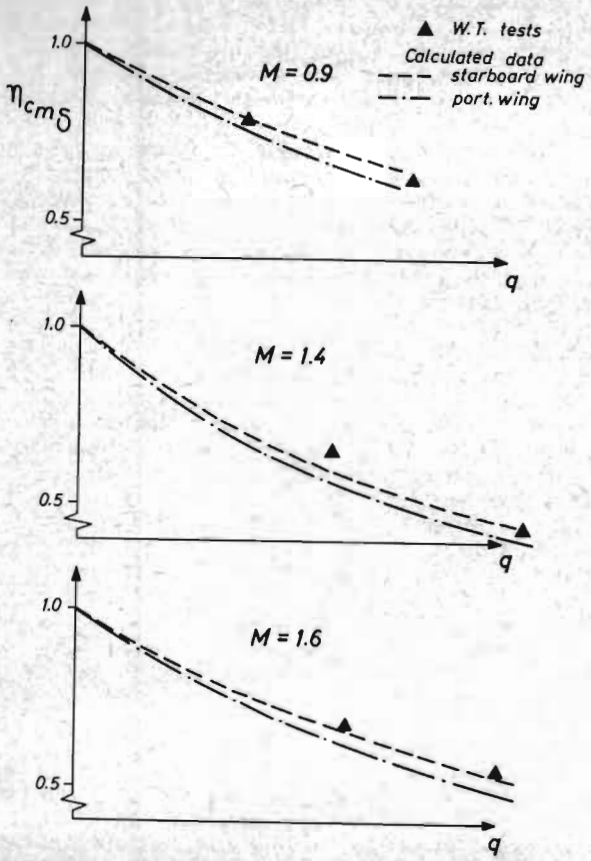

FIG. 11 COMPARISON BETWEEN COMPUTATIONS AND WINDTUNNEL TESTS

The result of such a correction, applied to data from windtunnel tests with a rigid model, is compared in Figure 12 with data from tests with an elastic model. The η -values that were used were computed for the elastic windtunnel model itself. The comparison shows that the non-linearitics are adequately reproduced.

Figure 13 shows an example of the variation of η through the transonic speed range. It is clear that the windtunnel test results are of essential importance. The sharp drop in η between M=.9 and M=1 would be hard to predict without these test results.

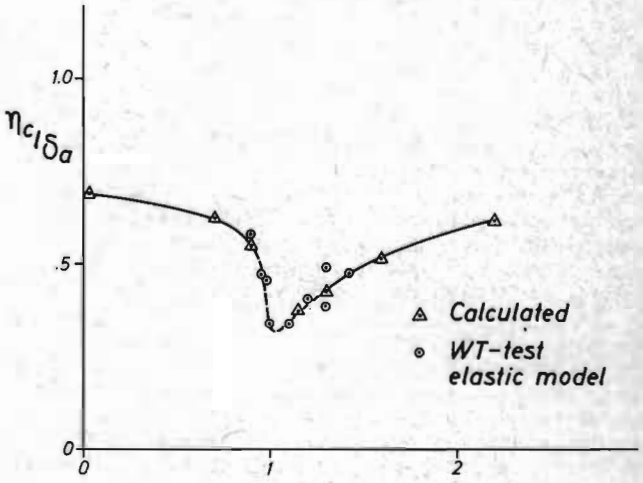

FIG. 13 INTERPOLATION THROUGH THE TRANSONIC SPEED RANGE AIDED BY WINDTUNNEL TESTS

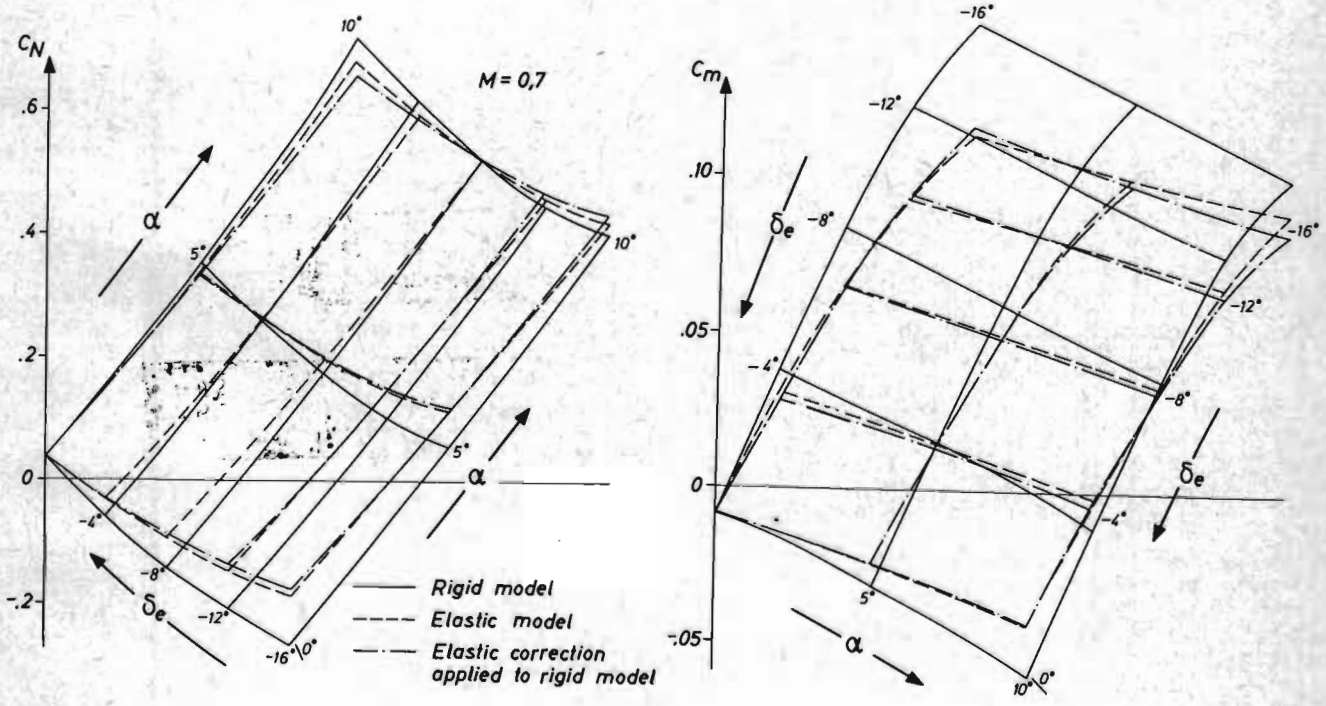

FIGURE 12. COMPARISON OF ELASTIC MODEL WT-RESULTS WITH CORRECTED RIGID MODEL DATA

The results of the windtunnel tests with elastic models, although not directly used as aerodynamic data for the aircraft, thus gave a valuable check on the computation of the η -values, showed that non-linearities could be treated by combining rigid model results with η -values and, last but not least, provided the possibility of interpolating through the transonic speed range.

Flight test results

For the aircraft, η -values for all aerodynamic derivatives were, to begin with, computed using a computed deformation matrix. As soon as aircraft hardware became available, the deformation matrix was experimentally checked for the canard, wing, elevon, fin and rudder.

The combination of main wing and elevon posed a special problem because of the way the control system commands the elevons, see Figure 14. The inner elevon, which has two hydraulic jacks, receives the pilot commands at the valve on the inner jack, while the outer jack receives the same hydraulic pressure as the inner one. The outer elevon, with one hydraulic jack, is slaved to the outer jack on the inner elevon. The deformation of the elevons under loads is thus appreciably different from what it would be if the jacks were replaced by springs with the right stiffness as was done in the windtunnel tests. Flight test results regarding elevon effectiveness are therefore not directly comparable with windtunnel test results.

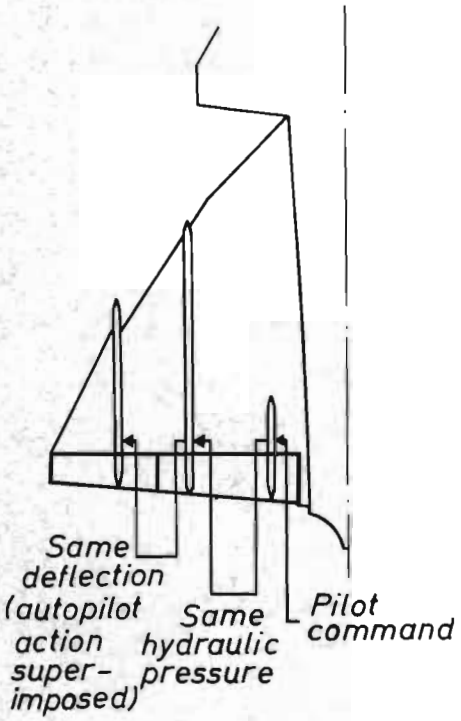

FIG. 14 ELEVON COMMAND SYSTEM

As Maxwell's theorem is not longer valid for this part of the system, interpolations and combinations have to be executed with care. As a check, some deformation measurements were done on an aircraft with an activated control system.

In flight tests, aerodynamic derivatives are obtained from taperecorded time-histories of aircraft movement in response to control surface pulses. After extensive checking of attitude angles, angular velocities, angle of attack and yaw, linear accelerations and speed against each other and after introduction of the necessary corrections, sets of equations are formed for ΔC_N , ΔC_T , ΔC_c , ΔC_m , ΔC_n and ΔC_ℓ (Δ -values from the trimmed condition before the control surface pulse). These equations, one set for each sample from the time history, that can be sampled at a rate of 25 samples/second, contain 70 unknown aerodynamic derivatives. After reducing this number to 23 by eliminating the crossderivatives containing both α and β , using windtunnel data, the equations, which, with a maximum number of 75 appreciably outnumber the unknowns, are solved by the method of least squares to obtain unique values of the derivatives. In the lateral case, where the equations are poorly conditioned, a weighting process is necessary to obtain the derivatives with acceptable accuracy.

As a final check, the derivatives are used in a 6 degrees of freedom digital simulation with the flight test control surface pulse as input and the computed aircraft movement is compared with the flight test measurements.

The whole method is described in more detail in ref 3.

As the flight tests were mainly performed at the standard altitudes of 1, 6 and 11 km, curves were prepared showing computed derivatives as a function of Mach number at these altitudes to enable direct comparison with flight test results. Figure 15 shows such curves together with the "rigid" curve from windtunnel tests for elevon-aileron- and rudder effectiveness, three derivatives with appreciable aeroelastic effects. The flight test results are plotted in and show fully satisfactory agreement. Generally, the agreement between predicted and flight tested data is good for all derivatives for which a reliable "rigid" prediction could be obtained. Use of the fairly simple methods for computation of aeroelastic effects as described in this paper thus resulted in a prediction of aerodynamic data with for design purposes fully adequate accuracy.

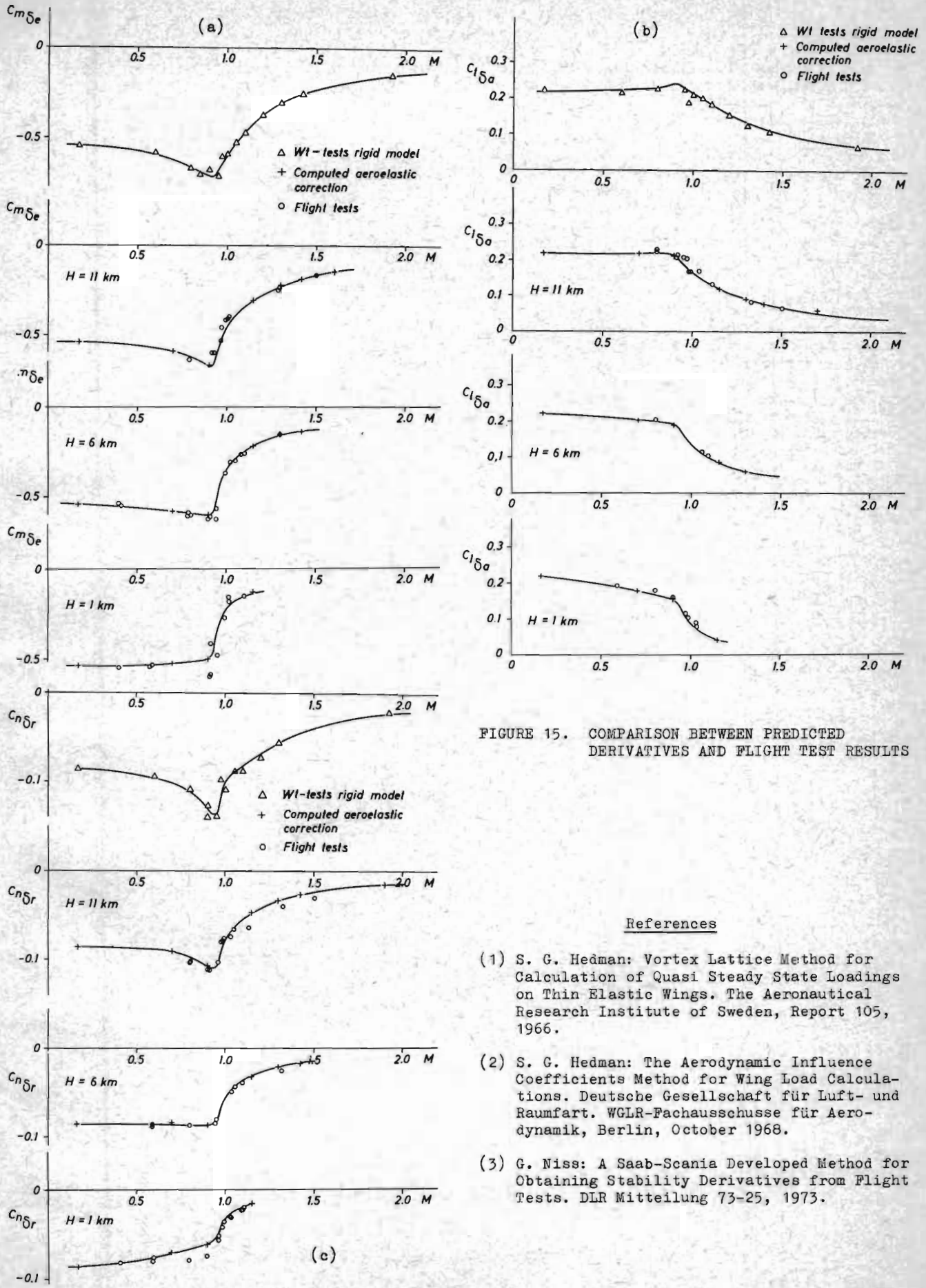

FIGURE 15. COMPARISON BETWEEN PREDICTED DERIVATIVES AND FLIGHT TEST RESULTS

References

(1) S. G. Hedman: Vortex Lattice Method for Calculation of Quasi Steady State Loadings on Thin Elastic Wings. The Aeronautical Research Institute of Sweden, Report 105, 1966.

(2) S. G. Hedman: The Aerodynamic Influence Coefficients Method for Wing Load Calculations. Deutsche Gesellschaft für Luft- und Raumfart. WGLR-Fachausschusse für Aerodynamik, Berlin, October 1968.

(3) G. Niss: A Saab-Scania Developed Method for Obtaining Stability Derivatives from Flight Tests. DLR Mitteilung 73-25, 1973.

D I S C U S S I O N

R. Legendre (ONERA, Chatillon, France): I shall raise a question of the same kind as the question raised by Dr. W.R. Jones during the discussion of the previous paper.

Using the linear theory, you cannot take into account the effects of the rolling up of the vortex sheet. In the case of the Viggen, I think the effects of this rolling up may be important as the front wing is near the other. I suppose the pressure distribution is modified, but the aeroelastic influence damps the fluctuation as it is an integrated result.

J. Kloos and S.G.L. Elmeland: You are right in supposing that the effect of the rolling up of the vortex sheet is important for the pressure distribution. The integrating effect of the η-calculation is clearly demonstrated in figs 7 and 8 for the transonic case. This effect, together with the way the η-values are defined and used (see eq. 11 and fig. 12) makes linear theory adequate even when non-linearities occur.